CORROSION IN VOLCANIC GASES

Keith A Lichti, Susan J Swann and Stephen P White
Materials performance Technologies, Industrial Research Limited, New Zealand

Norio Sanada, Yoshiaki Kurata, Hiroshi Nanjo and Jun Ikeuchi
Tohoku National Industrial research Institute, AIST, MITI, Japan

Bruce W Christenson
Institute of Geological and Nuclear Sciences, New Zealand

ABSTRACT

Volcanic gas environments on White Island, New Zealand, and Kuju-Iwoyama, Kyushu, Japan, have been used to study the corrosion properties of materials which might be used for engineering plant for energy production from deep-seated and magma-ambient geothermal systems. The corrosion chemistry of gases derived from natural volcanic features varies, from being no more aggressive than conventional geothermal fluids, to being so aggressive that only highly alloyed and expensive materials show suitable resistance. Models of corrosion product phase stability for common alloy elements contained in engineering alloys have been developed for gaseous environments using thermodynamic principles and conventional corrosion theory. These models give reasons for the observed corrosion kinetics and can be used to help to predict the performance of other alloys in similar environments. Deficiencies in the knowledge base for selection of materials for aggressive geothermal environments are identified, and directions for future research on materials having suitable corrosion resistance for anticipated deep-seated and magma-ambient production fluids are proposed.

INTRODUCTION

Research on the performance of materials in aggressive deep-seated geothermal production fluids has been limited because of the availability of wells capable of safely producing such fluids over a reasonable period of time for materials exposure tests. Natural volcanic features such as high temperature fumaroles and hot pools provide reasonable interim test sites for such work.

In New Zealand, a joint Japan/New Zealand initiative began the testing of materials in natural volcanic features on White Island in 1993 (Kurata et al, 1994, Kurata et al, 1995, Lichti et al, 1996). White Island was chosen for its relative ease of access and variety of environments available within a single site. The materials tests involved the direct exposure of metal samples in the volcanic features, and in tests in open fumaroles this resulted in inclusion of air in the test environments.

In Japan, corrosion studies in volcanic environments were initiated in 1992 at Kuju-Iwoyama in Kyushu, as part of a series of activities aimed at demonstrating the feasibility of producing energy from such environments (Ehara, 1994). The geothermal environment was derived from a shallow borehole drilled into a fumarolic area and cased with a 2 inch carbon steel pipe. The discharge gases were directed into an insulated test chamber where the metal specimens were held on exposure racks (Saito et al, 1994). The test arrangement gave a non-aerated superheated gas environment.

Volcanic gas environments, such as those encountered in fumaroles, have aggressive chemistries due to the presence of corrosive gases SO_2, H_2S, HCl and HF. Corrosion chemistries of such mixed gas environments have recently been characterised for iron, in an attempt to rationalise differences observed in corrosion kinetics between aerated and non-aerated corrosion test environments (Lichti et al, 1996). This paper reviews corrosion kinetic data obtained for these differing environments and extends the thermodynamic models for other alloying elements to describe the performance of common engineering alloys in gaseous fumarolic environments. A later paper will consider corrosion results and models of corrosion in hot pool-type liquid volcanic environments.

VOLCANIC GAS TEST SITES

The test sites used for corrosion studies on White Island included a high-temperature fumarole, WI #9 (Noisy Nellie) and a low-temperature fumarole, WI # 12 (Table 1). Exposed samples were placed directly into the open fumaroles for the duration of the test periods. WI #9 (Noisy Nellie) is of large diameter, >15 m and depth, >12 m, while WI #12 is about 1.5 m in diameter and about 1 m deep.

Over the three year period of tests, a number of differing environments were encountered in WI #9 (Noisy Nellie), these included (Table 1):

- a period of stable high temperatures in the range 230 °C to 190 °C, dry superheated gas, aerated
- a period of lower temperatures apparently below the dew point for the gas mixture, wet gas, aerated
- a period of very low temperatures in the base of the fumarole where the metal samples were exposed at 19 °C to 114 °C, very wet gas, aerated.

Testing of metals in a fumarolic environment on Kuju-Iwoyama in Japan (see Table 1) was done by drilling a small bore hole below an area where significant fumarolic activity was observed. The hole intersected what appeared to be a feed zone and gave single phase superheated steam at a temperature of 233 °C. The tests were conducted in an insulated metal chamber at atmospheric pressure with steam feed taken directly from the discharge pipe, and hence it is believed that air was excluded from this nominally dry gas test environment.

Table 1- Volcanic gas environments used for corrosion tests.

Exposure Site	Start Date	Temperature	Comments
High-temperature fumaroles		°C	
White Island #9 (Noisy Nellie)			Atmospheric Pressure
(Exposures Directly In Fumarole)			Natural Aeration
- 1st test - Coupons + SCC - 111 days	14.01.94	230 to 190	Dry Gas Environment
- 2nd test - Coupons - 7 days	21.02.95	95 to 145	Acid Formation Evident
- gas sampling	21.02.95	192	Dry Gas Sampled
- 3rd test - Coupons + SCC - 44 days	28.02.95	90 to 119	Acid Formation Evident
- 4th test - Coupons *	14.02.96	19-114	Condensation Evident
- gas sampling	14&17.02.96	120	Limited Gas Discharge
Kuju-Iwoyama			Atmospheric Pressure
(Exposures In Insulated Steam Chamber)			Non-aerated Steam/Gas Taken
Coupons + SCC - 10 months	27-12-92	230	From Fumarole Area Borehole
Low-temperature fumarole *			
White Island #12			Atmospheric Pressure
(Exposures Directly In Fumarole)			Natural Aeration
- 1st test - Coupons - 111 days *	15.01.94	98	Sulfur Precipitation Evident
- 2nd test- gas sampling + SCC - 30 days *	21.02.95	98	Sulfur Precipitation Evident

* The results obtained in these low temperature tests will be the subject of a future paper.

The geochemistry of the test sites on White Island and on Kuju-Iwoyama are summarised in Table 2 (Lichti et al, 1996). These chemistries are similar to those derived from other volcanic fumaroles (see for example, Giggenbach et al, 1990), and also show some similarities to gases derived from aggressive geothermal wells, in for example, the Philippines (Maturgo, 1996, Salonga, 1996).

Table 2- Geochemistry of Fumarole Environments Used for Corrosion Testing (Lichti et al, 1996).

Location	Date	T	CO_2	H_2S	SO_2	NH_3	HF	HCl	CO	H_2	O_2*	N_2	CH_4	Ar	H_2O	Gas*
		°C	mmol gas/100 mol gas plus steam													wt%
WI #9[1]	15.6.88	280	425	82.6	309	0.23	0.25	5.33	0.002	34.8	-	4.36	4.55	0.03	99134	2.3
WI #9[2]	21.2.95	193	1381	94.3	133	15.5	3.87	35.1	-	43.1	(62.8)	119	5.48	0.90	98169	4.3
WI #12[2]	15.1.94	98	9171	53.7	40.0	0.07	0.07	0.94	-	0.07	(0.13)	69.1	16.2	0.11	90649	22.8
Kuju-Iwoyama[3]	27.12.92	230	1400	750	240	-	10.0	30.0	-	-	-	-	-	-	97580	5.8

* O_2 in original samples, results shown are corrected for air contamination; **Total Gas in Steam
[1] Giggenbach and Sheppard, 1989; [2] Lichti et al, 1996; [3] Saito et al, 1994

CORROSION OF ENGINEERING ALLOYS IN VOLCANIC GASES

Engineering alloys as described in Table 3 were exposed in the differing tests in volcanic gases on White Island (Kurata et al, 1994, Kurata et al, 1995) and Kuju-Iwoyama (Saito et al, 1994). The tests cover a range of high temperature dry gas environments, both aerated and non-aerated, and wet (condensate containing) aerated environments as outlined in Table 3. Evaluated surface corrosion and stress corrosion cracking results are summarised in Table 4. Table 5 gives a summary of analysis results for corrosion products formed in the differing environments.

The surface corrosion rate and stress corrosion cracking results indicate:

- low rates of surface corrosion in the dry non-aerated superheated gas (Table 4 - Kuju-Iwoyama, Coupon samples)
- metal sulfide and hydrated ferrous sulfate corrosion product stability in the dry non-aerated superheated gas (Table 5 - Kuju-Iwoyama, Coupon samples)
- high rates of surface corrosion in the dry aerated superheated gas (Table 4 - White Island, Coupon samples)
- metal oxide and metal chloride corrosion product stability in the dry aerated superheated gas (Table 5 - White Island, Coupon samples)
- high rates of surface corrosion in the wet aerated gas (Table 4 - White Island, Coupons and U-Bend samples)
- stress corrosion cracking of types SUS304 and 316 stainless steels in dry non-aerated superheated gas (Table 4 - Kuju-Iwoyama, Bent Beam samples)
- stress corrosion cracking of types SUS304 and 316 and the duplex alloy 22Cr-5Ni in wet aerated gas (Table 4 - White Island, U-Bend samples)
- an absence of coherent corrosion products in wet aerated gas with an oily film containing high concentrations of dissolved metal ions and contaminant corrosive ions (Table 5 - White Island, U-Bend samples)
- significant cross contamination of corrosion products (see FeS_2 on A-5083 aluminium alloy and contaminant metal ions on Ti alloys in Table 5). (Note that the all U-Bend materials except the Ti alloys were stressed using straps made from Alloy 1925hMo fixtures and corrosion product from this material is entrained in the wash water samples for these alloys.)
- $CaSO_4$ precipitation in the dry gas environments (Table 5 - White Island and Kuju Iwoyama, Coupons and Chamber Wall)

MODELS OF CORROSION IN VOLCANIC GASES

1. Dry gas environments

The corrosion chemistry of dry superheated high temperature gas fumarole environments can be described using phase stability diagrams for metals and metal reaction compounds as a function of log pSO_2 vs log pO_2 (Lichti et al, 1996). Figure 1 shows a series of such diagrams for the alloying elements iron, nickel, chromium, molybdenum and titanium as well as a phase stability diagram for nickel as a function of log pCl_2 vs log pO_2. Equilibrium phase stability calculations suggest the conditions in the White Island and Kuju-Iwoyama test sites had similar pSO_2 at 10^{-3} atm but had differing pO_2 values, Noisy Nellie, 10^{-3} atm and Kuju-Iwoyama, 10^{-33} atm (Lichti et al, 1996). The pCl_2 in these environments was calculated to be 10^{-22} atm when pHCl was 10^{-3} atm. The diagrams were constructed using thermodynamic data extracted from the Outokumpu HSC Chemistry database.

Reactions of the WI #9 (Noisy Nellie) and Kuju-Iwoyama fumarolic gas mixtures with iron are illustrated on the Fe-S-O diagram of Figure 1. The air-free and air-in-equilibrium gas mixtures have partial pressures which stabilise layers of Pyrite (FeS_2) and Troilite (FeS) or Pyrrohotite ($Fe_{(1-x)}S$) as the metal surface is approached from the metal sulfide/gas interface. The non-equilibrium air-containing gas has a range of possible concentrations which coincide with ferrous and ferric sulfates and Hematite (Fe_2O_3) and Magnetite (Fe_3O_4) forming on the metal surface. The predicted sulfide stability on carbon steel samples is confirmed for the Kuju-Iwoyama tests, Table 5 (Saito et al, 1994) while oxide stability was observed on tests in WI #9 (Noisy Nellie) at these temperatures, Table 5 (Kurata et al, 1995). Kuju-

Table 3- Metals and Alloys Tested for Resistance to Corrosion on White Island, WI (Kurata et al, 1995) and Kuju-Iwoyama, K-I (Saito et al, 1994).

Material Type	UNS No.	Normal Composition	Dry Gas		Wet Gas	Low T *
			WI#9	K-I	WI #9	WI #12
Carbon and Low Alloy Steels						
SS400	---	Carbon steel	C	C	C	C
Cast Iron	---			C		
SMA49AW	---	Cor-Ten		C		C
N80	---	API standard	C			C
L80	---	API standard	C			C
CrMoV	---	Low Alloy Steel		CB		
2.5Ni	---	Low Alloy Steel		CB		
Ferritic and Martensitic Stainless Steel						
SUS405	S40500	12Cr		CB		
13Cr	S41000	13Cr	C			C
13CrMo	---	13Cr-1Mo		CB		
23Cr-6Al	---	23Cr-6Al	C			
17-4PH	S17400	17Cr-4Ni-4Cu-0.3Cb		CB		
Austenitic Stainless Steels						
SUS304	S30400	18Cr-8Ni	CW	CB	CWU	CU
SUS304L	S30403	18Cr-8Ni-0.03C		CB		
SUS316	S31600	18Cr-10Ni-2.5Mo	CW		CW	C
SUS316L	S31603	18Cr-10Ni-2.5Mo-0.03C		CB	U	U
Duplex Stainless Steels						
22Cr-5Ni	S31803	22Cr-5Ni-3.0Mo-0.15N	CW		U	CU
25Cr-7Ni	S32750	25Cr-7Ni-3.5Mo-0.01N	CW	CB	C	C
25Cr-7Ni-N	S32750	25Cr-7Ni-3.5Mo-0.02N	CW			
High Alloy Stainless Steels and Nickel Base Alloys						
SS 2562 (904L)	N08904	19.5Cr-25Ni-4.5Mo-1.5Cu	CW		CWU	CU
254 SMO	S31254	21Cr-17Ni-6Mo-0.6Cu-0.2N			U	U
1925hMo	N08926	21.5Cr-25Ni-6Mo-1Cu	CW		CU	CU
Alloy 28	N08028	27Cr-31Ni-3.5Mo-1Cu			U	U
Alloy 600	N06600	16Cr-73Ni-9.5Fe			U	U
Alloy 601	N06601	23Cr-63Ni-13Fe			U	U
Alloy 625	N06625	21.5Cr-61Ni-9Mo-2.5Fe-3.7(Nb + Ta)	CW		CU	CU
Alloy 690	N06690	30Cr-60Ni-9.5Fe-1(Nb + Ta)	CW			
Alloy 800	N08800	21Cr-32.5Ni-46Fe-0.04C	CW			
Alloy 825	N08825	21.5Cr-42Ni-3Mo-30Fe-2.2Cu-0.9Ti	CW		CU	U
Alloy 59	N06059	23Cr-59Ni-16Mo-1Fe	CW		CWU	U
Alloy 45TM	---	27Cr-47Ni-2.7Si-0.08N-Balance Fe	CW			
C 276	N10276	16Cr-55Ni-16Mo-6Fe-4W	CW		CWU	U
G 3	N06985	22.5Cr-43Ni-7Mo-20Fe-2Cu-Co	CW		CW	
Alloy 903	N19903	38Ni-15Co-3Nb-1.4Ti-0.7Al-0.01C	C			
Alloy B-2	N10665	69Ni-28Mo-1Cr(max)-2Fe(max)			CW	
Cobalt Alloy						
S 816	---	20Cr-20Ni-47Co-4Mo-4W-4(Nb + Ta)	C			
Aluminium Alloy						
Al Alloy	A95083	A-5083, 5Mg		CB		
Titanium Alloys						
Ti Grade 1	R50250	Ti(α)	CW		CW	
Ti Grade 4	R50700	Ti(α)			U	U
Ti Grade 5	R56400	Ti-6Al-4V	CW	CB	CWU	U

C = Coupon exposures for surface corrosion, W= Weld bead applied to coupons for Stress Corrosion Cracking test

B= Three point bending samples for Stress Corrosion Cracking tests

U= U-Bend stressed samples for Stress Corrosion Cracking tests (Surface corrosion by macroscopic measurements)

* The results obtained in these low temperature tests will be the subject of a future paper.

Table 4- Summary of Surface Corrosion and Stress Corrosion Cracking Test Results in Dry and Wet Gas Conditions (Kurata et al, 1995, Saito et al, 1994).

Material	Material Loss mm/y			Stress Corrosion Cracking		Material Loss mm/y			Stress Corrosion Cracking	
Environment	Dry Superheated Gas			Dry Superheated Gas		Wet Gas			Wet Gas	
Location	WI #9		Kuju-I	WI#9	Kuju-I	WI #9			WI #9	
Exposure Time	40 days	111 days	10 months	111 days	10 months	7 days	44 days	7 days	44 days	7 days
Aeration	Air	Air	No Air	Air	No Air	Air	Air	Air	Air	Air
Monitor (see Table 3)	C	C	C	W	B	C	C	U	W	U
Carbon and Low Alloy Steels										
Carbon Steel	0.707	0.735	0.038			35.4				
Cast Iron			0.042							
Cor-Ten			0.029							
N80	0.785	0.652								
L80	0.759	0.613								
CrMoV			0.029		No					
2.5Ni			0.027		No					
Ferritic and Martensitic Stainless Steels										
SUS405			0.021		No					
13Cr	2.236	2.112								
13CrMo			0.022		No					
23Cr6Al	3.048	2.922								
17-4PH			0.014		No					
Austenitic Stainless Steels										
SUS304(Annealed)	0.613	1.304	0.007	No	No	27.8	Lost	61	Lost	Severe
SUS304(650°Cx2hrs)			0.008		Yes-at 2 months					
SUS304L(Annealed)			0.006		Yes					
SUS304L(650°Cx2hrs)			0.006		No					
SUS316(Annealed)	0.466	1.086		No		21.3	Lost		Lost	
SUS316L(Annealed)			0.001		Yes			55		Severe
SUS316L(650°Cx2hrs)			0.001		Yes					
Duplex Stainless Steels										
22Cr-5Ni	0.907	1.327		No				60-117		Yes
25Cr-7Ni	1.082	1.389	0	No	No	34.0				
25Cr-7Ni-N	1.020	1.061		No						
High Alloy Stainless Steels and Nickel Base Alloys										
SS 2562 (904L)	0.601	0.650		No			Lost	29	Lost	No
254 SMO								29		No
1925hMo	0.243	0.309		No		19.4	11.2	35	No	No
Alloy 28								33		
Alloy 600								35		No
Alloy 601								43		No
Alloy 625	0.048	0.038		No		8.4		11		No
Alloy 690	1.879	0.933		No						
Alloy 800	1.278	1.263		No						
Alloy 825	0.903	0.506		No		16.4		29		No
Alloy 59	0.003	0		No			0.043	n.d.	No	No
Alloy 45TM	1.389	1.402		No						
C 276	0.013	0.016		No		7.7	5.85	20	No	No
G 3	0.123	0.162		No			8.5		No	
Alloy 903	0.358	0.409								
Alloy B-2							3.04		No	
Cobalt Alloy										
S816	0.142	0.068								
Aluminium Alloy										
A-5083			0.374		No					
Titanium Alloys										
Ti Grade 1	0	0		No			Gain		No	
Ti Grade 4								n.d.		No
Ti Grade 5	0	0	0	No	No		0.043	n.d.	No	No

n.d. = not detected

Table 5- Summary of Analysis of Corrosion Products Formed in Volcanic Corrosion Test Environments (Kurata et al, 1995, Saito et al, 1994).

Material	Dry Superheated Gas White Island Aerated	Kuju-Iwoyama Non-Aerated	Wet Gas White Island 95-145°C Contents of Washed "Oily" Films and Corrosion Products in 100 ml of Distilled and Deionised Water (mg/kg)								
			Fe	Ni	Cr	Cu	Mo	Cl	SO_4	F	pH
Carbon and Low Alloy Steels											
SS400, N80	Fe_2O_3, $CaSO_4$										
L80, 13 Cr	Fe_2O_3, $CaSO_4$										
23Cr-6Al	Fe_2O_3, $CaSO_4$										
CrMoV		FeS_2, $FeSO_4 \cdot 7H_2O$									
2.5Ni		FeS_2, $FeSO_4 \cdot 4H_2O$, $FeSO_4 \cdot 7H_2O$,	(38)					(0.3)	(9)		(3.1)
Austenitic Stainless Steels											
SUS304	Fe_2O_3		1900	630	250	420	4	2960	20	2	2.3
SUS316	Fe_2O_3										
SUS316L		FeS_2, $FeSO_4 \cdot 7H_2O$, $(Cu, Fe, Ni)S_2$	900	430	200	430	9	1800	55	3	2.4
Duplex Stainless Steels											
22Cr-5Ni	Fe_2O_3,FeOOH, $CaSO_4$		2080	480	290	420	7	3210	30	1	2.1
25Cr-7Ni											
SS 2562(904L)	Fe_2O_3, CrO_2		620	520	200	430	10	1650	75	2	2.5
High Alloy Stainless Steels and Nickel Base Alloys											
254 SMO			790	530	230	420	11	1840	110	8	2.4
1925hMo			640	500	230	420	12	1620	95	3	2.5
Alloy 28			460	610	180	430	8	1420	75	7	2.6
Alloy 600			350	2750	10	420	0	4210	25	0.4	2.7
Alloy 601			730	2450	530	420	3	3590	45	26	2.9
Alloy 625			230	840	150	420	6	1320	140	5	2.8
Alloy 690	$NiCl_2 \cdot 6H_2O$										
Alloy 800	$NiCl_2 \cdot 6H_2O$, Fe_2O_3										
Alloy 825	$NiCl_2 \cdot 6H_2O$,Fe_2O_3		470	730	180	410	9	1520	65	3	2.6
59			250	330	130	410	9	750	65	2	2.8
Alloy 45TM	$NiCl_2 \cdot 6H_2O$, $NiCl_2 \cdot 4H_2O$										
C276			140	430	60	430	1	750	90	3	2.8
G3	$Fe_2O_3CrO_2(SO_4)_3$, Ca_2SO_4										
Cobalt Alloy											
S816	$CoCl_2 \cdot 6H_2O$										
Aluminium Alloy											
A-5083		FeS_2									
Titanium Alloys											
Ti Grade 4			170	160	70	420	3	740	70	7	2.8
Ti Grade 5			130	120	40	420	1	470	60	5	2.8
SUS316L Chamber Wall		FeS_2, $CaSO_4$, α-S, $CaSO_4 \cdot 2H_2O$	(17)					(7.8)	(16)		(3.0)

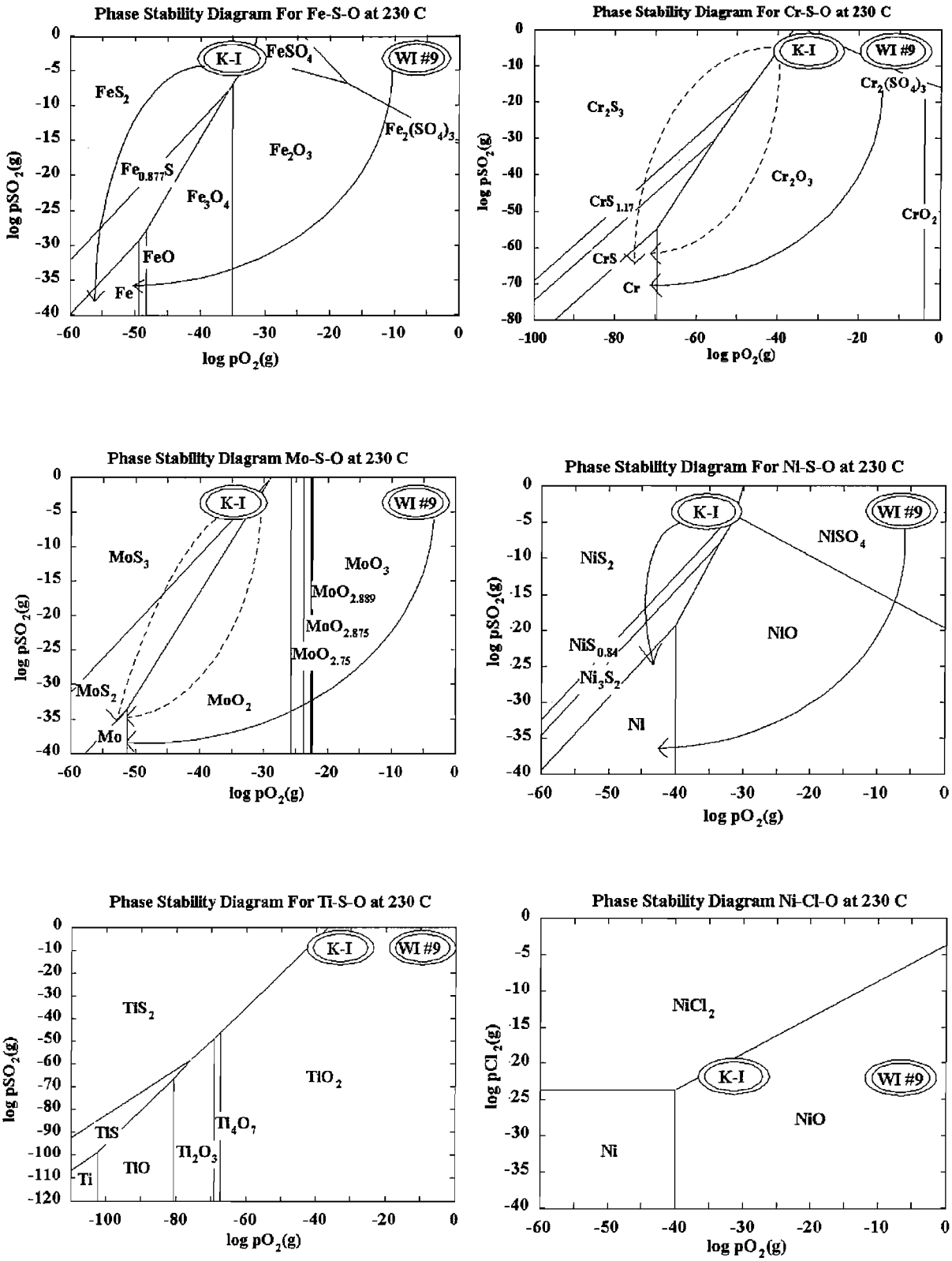

Figure 1- Phase stability diagrams for Fe, Cr, Ni, Mo and Ti in volcanic gases at 230°C. Arrows indicate possible reaction paths.

Iwoyama with low oxygen partial pressures gave iron sulfide stability and low corrosion rates (Tables 4 and 5) while exposure to air in WI #9 (Noisy Nellie) on White Island gave hematite stability and a high corrosion rate (Tables 4 and 5) (Lichti et al, 1996).

Figure 1 also shows the types of corrosion products which might be predicted to form on alloyed materials. Oxides of chromium and molybdenum would be expected in either the aerated and non-aerated dry gas environments. The corrosion results suggest $NiCl_2$ is more stable than the nickel oxides, sulfides and sulfates (compare Ni-Cl-O and Ni-S-O diagrams in Figure 1). In the aerated environments there is a marked decrease in corrosion as the molybdenum content of the stainless steels and nickel base alloys is increased, see Tables 3 and 4 (Kurata et al, 1995) and the phase stability diagram for Mo shows good stability of molybdenum oxides. The diagram for Ti suggests formation of stable protective films of Rutile (TiO_2) under all conditions. Dry gas models of the type shown in Figure 1 will be sufficient for initial predictions of corrosion in systems where steam superheat is maintained but will not apply when condensation occurs as the temperature is lowered.

2. Condensing acids/aqueous corrosion models

The "oily" liquid formed in WI #9 (Noisy Nellie) in the temperature range 95-145°C (Table 5) was rich in chloride ions and sulfate ions. Thermodynamic calculations have been done to determine the potential for H_2SO_4 condensation at temperatures above 100°C. The results indicate that this effect is unlikely to occur as the calculated maximum H_2SO_4 (g) partial pressure was 10^{-20} atm. The volcanic gases would not be expected to condense until the temperature approached the saturation temperature for water (100°C). Once saturation temperature is approached and steam condensate is formed then the HCl and HF in particular will readily partition into the condensed phase and even though the acids formed are relatively strong conventional aqueous corrosion models such as potential-pH Pourbaix diagrams can be used to describe the corrosion chemistry.

The aqueous corrosion properties of initially formed steam condensate in equilibrium with fumarole steam and gas has been estimated for the WI #9 (Noisy Nellie) fumarole chemistry given in Table 2, ie pH = 0.4 at Total S of 0.2689 mol/kg (Lichti et al, 1996). The potential-pH, Fe-S-H_2O stability diagram shown in Figure 2 describes the equilibrium thermodynamic conditions. The diagrams can not be used to make predictions of corrosion without confirmation of corrosion rates from in-situ tests, however it is clear that at pH less than about 4, carbon steels will not form passive films and will

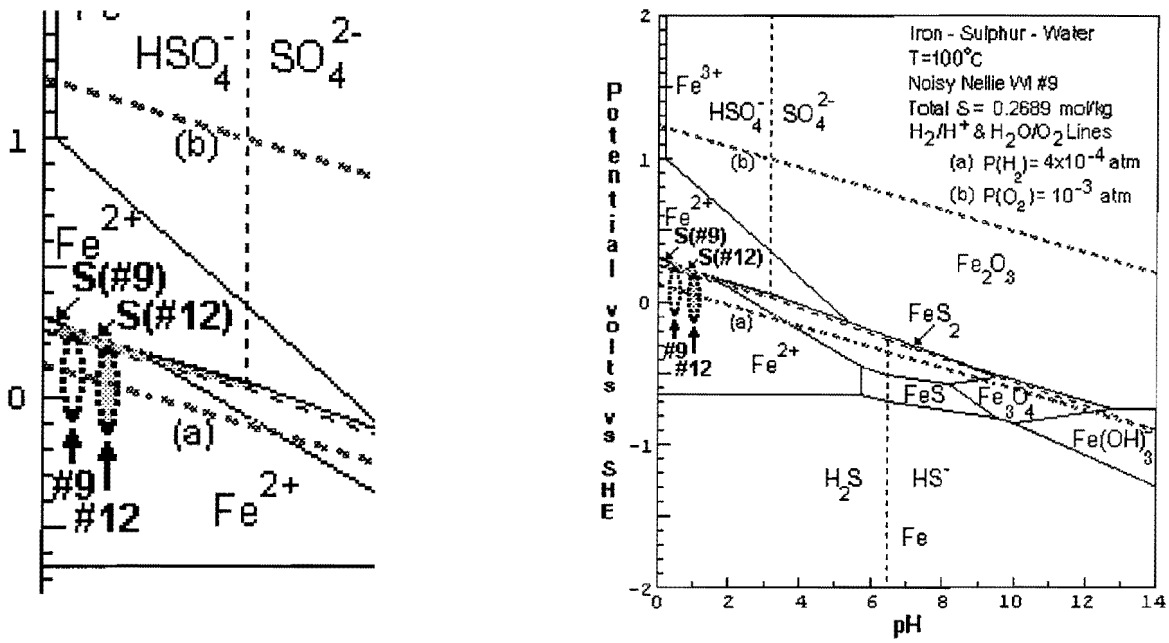

Figure 2- Potential-pH Fe-S-H_2O Diagram for Total S = 0.2689 mol/kg and T = 100 ° C (Lichti et al, 1996).

freely corrode. Table 4 indicates a high rate of corrosion even for stainless steels and in wet aerated conditions but again there is a decrease in corrosion for the more alloyed materials and for titanium. Potential-pH diagrams for Cr and Ni in high salinity brines containing significant concentrations of S suggest that these alloy elements will also readily dissolve in strongly acid condensates although titanium shows good passive film formation (MacDonald et al, 1979). Very high molybdenum alloy content materials, especially those which have almost no iron appear to give the best results of all the nickel base alloys tested ie Alloy B-2 and Alloy 59 (Table 4).

DEFICIENCIES IN MATERIALS KNOWLEDGE BASE

Specification of materials for reliable energy production from deep geothermal resources will require understanding of the corrosion chemistry and materials performance of the derived environments. This knowledge will be collected through the development of:

- models of the chemistry of possible deep-seated and magma-ambient production fluids
- scenarios for process and plant options for handling of aggressive fluids
- models for the derived fluid chemistries - thermodynamic and kinetic
- corrosion kinetic results and models for candidate engineering alloys
- thermodynamic models of corrosion for alloyed materials
- relationships between thermodynamics models and corrosion kinetic models.

The corrosion results described in this paper have progressed the latter three points in particular by developing an understanding of the predominant corrosion mechanisms encountered in natural volcanic environments. The effects of increased pressures and changes in temperature have not been fully explored but the models can be adapted so that some prediction of potential problem areas for full-size plant can be made. The results suggest the key areas of remaining research for steam-containing mixed gases SO_2, H_2S, HCl and HF, are in non-aerated environments where acid formation and condensate formation can occur (Table 6).

Table 6- Corrosion Results Matrix for Aggressive Geothermal Environments.

Environment	Conditions	Results	Models	Mechanisms
Dry Gas	T>200°C, Non-Aerated	Kinetics/SCC	Phase Stability Diagrams	Passive Films
Dry Gas	T>200°C, Aerated	Kinetics/SCC	Phase Stability Diagrams	Non-Protective Films
Wet Gas	T=100-200°C, Non-Aerated	None	Isocorrosion and	Potential for Acid Attack
Wet Gas	T=100-200°C, Aerated	Kinetics/SCC	Pourbaix Diagrams	Acid Attack
Wet Gas	T<100°C, Non-Aerated	None	Isocorrosion and	Potential for Acid Attack
Wet Gas	T<100°C, Aerated	Kinetics/SCC	Pourbaix Diagrams	Acid Attack

The corrosion results indicate care is required in the handling of aggressive geothermal fluids. In many "acid" wells encountered to date the produced fluids have been too aggressive to permit production, and the wells have either been used for reinjection or cemented shut. Materials which may have sufficient resistance can be selected from available results but care is required in the application of these alloys to new environments. Corrosion testing in two phase and liquid dominated systems such as has been completed for HCl containing environments (Sanada et al, 1995) will be required.

Significant effort is also required to progress the first three points noted above in order to refine the developed models of corrosion and the understanding of the corrosion mechanisms. The drilling and production of more deep-seated wells will provide information on the geochemistry of these fluids and will allow refinement of the models. Ideally, in-situ corrosion tests can be scheduled for these new wells so that the preferred materials can be further tested. Additional chemical data will also provide input for determining the best process and plant options which will optimize energy recovery, while minimising the size of plant which must be constructed of more expensive, corrosion resistant materials.

CONCLUSIONS

Volcanic gas environments which are dry as a result of significant superheat give low rates of corrosion on carbon and low alloy steels and stainless steels, so long as they are kept air free. Introduction of air changes the stability of corrosion products, from protective sulfide films to non-protective oxides and

and susceptible materials readily corrode. Loss of superheat and formation of acid condensate have been shown to further accelerate corrosion in the aerated environments.

Models of corrosion for common alloy elements contained in engineering alloys have been developed for gaseous volcanic environments using thermodynamic principles and conventional corrosion theory. These models confirm the stability of formed corrosion products, and give reasons for the observed corrosion kinetics. The models can be used to help to predict the performance of other alloys in similar environments.

Deficiencies in the knowledge base for selection of materials for aggressive geothermal environments include wet non-aerated environments, particularly those which will be formed in heat exchange situations when the fluids are under pressure.

ACKNOWLEDGEMENTS

The authors acknowledge the financial support of the New Zealand Foundation for Research Science and Technology and the AIST, MITI, Japan in the preparation of this paper. Testing on White Island was done with permission of Mr J R Buttle.

REFERENCES

Ehara, S. (ed) (1994). Field study of power generation by using volcanic geothermal reservoir, Report of the Grant in Aid on General Research Supported by the Ministry of Education Science and Culture, Japan, 19 Sept (in Japanese).

Giggenbach, W.F., Gaecia, N., Londono C., A., Rodriguez V., L., Rojas G., N., and Calvache V., M.L. (1990). Jnl of Vol and Geothermal Res, 42, pp. 13-39.

Giggenbach, W.F. and Sheppard, D.S. (1989) Variations in the temperature and chemistry of White Island fumerolic discharges 1972-85, In NZ Geological Survey Bulletin 103, pp 119-126.

Kasai, K., Miyazaki, S., Sasaki, M., Yagi, M. and Uchida, T. (1996). Supersaline brine in the Kakkonda granite obtained from WD-1A in the Kakkonda Geothermal Field, Japan, in Proc VIIIth Int Symp on the Observation of the Continental Crust Through Drilling, Tsukuba, Japan, Feb 26 to Mar 2, pp359-364.

Kurata, Y., Sanada, N. Nanjo, H., Ikeuchi, J. and Lichti, K.A. (1995). Material damage in a volcanic environment, World Geothermal Congress, Milan, Italy, May, pp 2409-2414.

Kurata, Y., Sanada, N. Nanjo, H., Ikeuchi, J. and Lichti, K.A. (1994). Field testing of materials at White Island, in Extended Abstracts of Workshop on Deep-seated and Magma-Ambient Geothermal Systems, Tsukuba, Japan, Mar, pp 167-170.

Lichti, K.A., Gilman, N.A., Sanada, N., Kurata, Y., Nanjo, H., Ikeuchi, J. and Christenson, B.W. (1996). Corrosion chemistry of some volcanic environments, in Proc of 18th New Zealand Geothermal Workshop, Nov, U of Auckland, pp 21-28.

Lichti, K.A. and McIlhone, P.G.H. (1994). Materials for volcanic environments, Where will the data come from, in Proc 16th NZ Geothermal Workshop, Geothermal Institute, U of Auckland, Nov, pp 35-40.

MacDonald, D.D., Syrett, B.C. and Wing, S.S., (1979) The use of Potential-pH diagrams for the interpretation of corrosion phenomena in high salinity geothermal brines, Corrosion, Vol 35, No 1, Jan, pp 1-11.

Maturgo, O.O. (1996) Chemical characteristics of acid fluids in some PNOC geothermal wells, 17th PNOC-Energy Development Corporation Geothermal Conference, Manila, Philippines, pp111-117.

Outokumpu HSC Chemistry for Windows, (1994) Outokumpu Research Oy, Finland.

Sanada, N., Kurata, Y., Nanjo, H. and Ikeuchi, J. (1995). Material damage in high velocity acidic fluids, Geothermal Resources Council Transactions, Vol 19, Oct, pp.359-363.

Saito, M., Takano, Y., Saito, S. and Kondo, T. (1994) Field testing of materials at Kuju-Iwoyama solfatara, in Extended Abstracts of Workshop on Deep-seated and Magma-Ambient Geothermal Systems, Tsukuba, Japan, Mar, pp 189-199.

Salonga, N.D. (1996) Fluid and mineral equilibria in acid NaCl(+SO_4) reservoir: The case of Sandawa collapse, Mt Apo hydrothermal system, 17th PNOC-Energy Development Corporation Geothermal Conference, Manila, Philippines, pp 119-129.